Chapter 5

A Review of Climate Signals as Predictors of Long-Term Hydro-Climatic Variability

Shahab Araghinejad and Ehsan Meidani

Additional information is available at the end of the chapter

http://dx.doi.org/10.5772/56790

1. Introduction

1.1. Large scale climate signals

In many parts of the world coupled oceans atmospheric phenomenon provide important predictive information about hydrologic variability. Therefore, studying the relationships of these large scale features of the atmosphere with hydroclimatic events is helpful in hydrological and meteorological long-lead forecasting, promoting awareness about climate variability, and water resources management. As the time scale over which the oceans respond are slower than atmosphere, efforts have been focused mostly on investigating the links of sea surface temperatures (SSTs) and sea level pressures (SLPs) of oceans with atmospheric changes for climate monitoring or use as potential hydro-climatic predictors.

This chapter reviews the characteristics of several widely known teleconnection indices and their effects on different regions of the world. The goal is to present basic information that might be useful for analysis and study of teleconnections. Knowledge concerning the contemporary dynamics of these teleconnections is essential contextual information against which the manifestations and impacts of future climate change can be assessed. For example, climate change is likely to change the intensity, timing, positional loci, as well as associated impacts of some of these teleconnections. The ability to assess such changes with a degree of accuracy is possible only if we have detailed information regarding past patterns of behavior.

2. El Niño Southern Oscillation (ENSO)

El Niño is one of the largest oscillations of the climate system and is defined as warmer than normal condition of Pacific Ocean surface temperature in tropical eastern parts (Figure

1).Under normal conditions, Pacific Ocean currents are east-to-west on the equator, causing the upwelling of deeper water toward the surface in the eastern parts. Every 2 to 7 years this westward flow weakens and reverses to an eastward flow of water called equatorial Kelvin waves. This abnormal condition is El Niño (warm phases) and typically can last for a duration of few months or more. La Niña episodes (cool phases) follows El Niño ones and alter the situation to normal and affect a global atmospheric pressure variation called the Southern Oscillation (SO), leading to the widely used term ENSO. Properties of ENSO are shown briefly in Table 1.

Climate signal	Region of occurrence	Indicator Index	Threshold	Phase persistence
ENSO	Equatorial Pacific Ocean	SOI	+/- 8	6-18 months
		Nino 1+2	+/- 0.5	
		Nino 3		
		Nino 3.4		
		Nino 4		

Table 1. The ENSO properties in brief

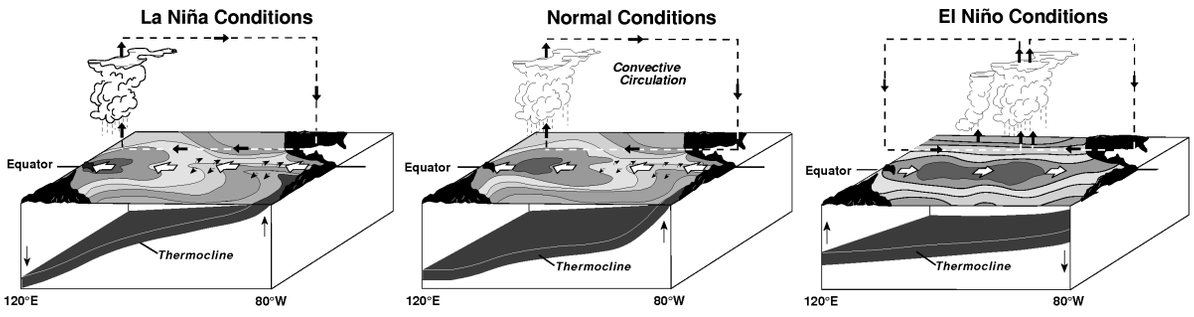

(Source:NOAA / PMEL / TAO Project Office, Dr. Michael J. McPhaden, Director, http://www.pmel.noaa.gov/tao/elnino/el-nino-story.html)

Figure 1. Schematic diagram of ENSO climate pattern in the Pacific Ocean

ENSO is one of the most widely studied large-scale climatic variability that affects temperature and precipitation in regions all over the globe. Dettinger and Diaz (2000) showed that these large-scale tropical fluctuations yield similarly global-scale fluctuations on streamflow and that streamflow teleconnections are as pervasive as meteorological teleconnections. Based on studies of 1345 sites around the world, El Niño variations have been found to correlate with streamflow in many parts of the Americas, Europe and Australia (Dettinger and Diaz, 2000). The effects differ significantly by location, as abundant rains become scarce in some areas while other areas experience flooding (Figure 2). For instance, El Niño episodes are accompanied by reduction in winter and spring rainfall over much of eastern Australia and the higher latitudes and La Niña increases the probability of eastern and northern Australia being wetter than normal (Power et al. 2005).

http://dx.doi.org/10.5772/56790

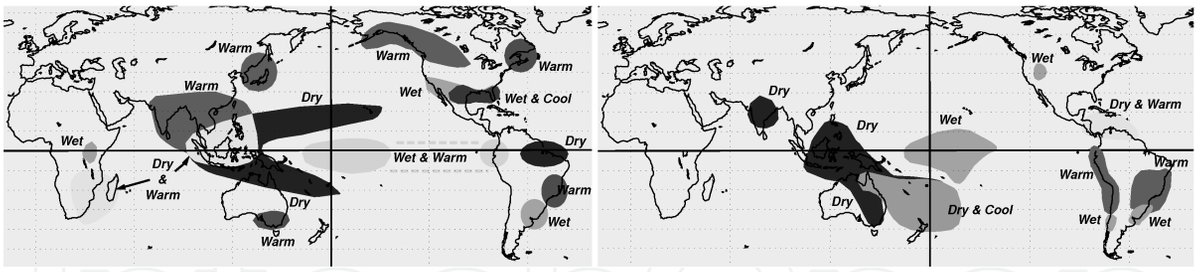

Figure 2. The regions having greatest impacts of El Niño during (*left*) December-February and (*right*) June-August. (Source: NOAA / PMEL / TAO Project Office, Dr. Michael J. McPhaden, Director, http://www.pmel.noaa.gov/tao/elnino/el-nino-story.html)

Currently, there is no single data set universally accepted for measurements of ENSO (Beebee and Manga 2004). Commonly used ENSO indices include regional SST indices (e.g., Nino-1+2, Nino-3, Nino-4, Nino-3.4) and SOI.

2.1. Nino index

These indices are based on the average sea surface temperature anomalies of the following regions and include, Niño 1+2 (0-10° S and 80-90° W), Niño 3 (5°N-5°S and 90-150°W), Niño 4 (5°N-5°S and 160°E-150°W) and Niño3.4 (5°N-5°S and 170-120°W) (Figure 3).

The raw values of the index are available from the Climate Prediction Center of The National Oceanic and Atmospheric Administration (NOAA) (http://www.cpc.ncep.noaa.gov/data/indices/) which is produced by using Reynolds OISST.v2 data from 1982 to present. When the index is positive then the temperature of the Pacific Ocean water is warmer than normal in the Nino regions and when the index is negative then water temperatures are cooler than normal. An El Niño or La Niña event is identified if, for example, the 3-month running-average of the NINO3.4 index exceeds +0.5°C for El Niño or -0.5°C for La Niña for at least 5 consecutive seasons. For example, El Niños occurred in 1982-83, 1986-87 and 1997-98 (Figure 4).

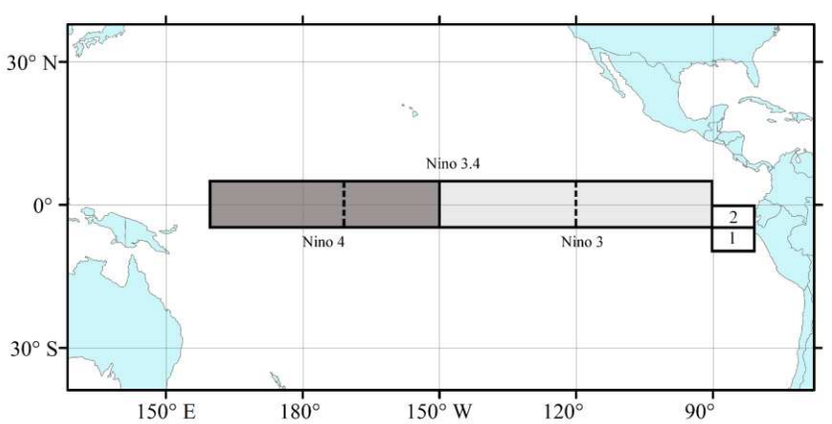

Figure 3. Pacific Ocean and corresponding Nino regions

2.2. Southern Oscillation Index (SOI)

SOI is an atmospheric pressure based index and is calculated using the pressure differences between Tahiti (17° 52' 0" south and 149° 56' 0" west) and Darwin (12° 27' 56" south and 130° 50' 33" east).

Positive values of SOI indicate strong trade winds in the tropics and the tropical Pacific. SOI data are available since late 19th century to present from the Australian Bureau of Meteorology website (http://www.bom.gov.au/climate/enso/).Sustained negative values of the SOI greater than −8 often indicate El Niño episodes and conversely, sustained positive values greater than +8 are typical of a La Niña episode. The 5-month running average of the SOI values also has been used as indicator of the episodes.

There are a few different methods for calculating the SOI. The method used by the Australian Bureau of Meteorology is the Troup SOI which is the standardized anomaly of the Mean Sea Level Pressure difference between Tahiti and Darwin. It is calculated as follows:

$$\mathrm{SOI} = \frac{(P_{diff} - P_{diffav})}{SD(P_{diff})} \tag{1}$$

Where: P_{diff} is the average Tahiti MSLP (mean sea level pressure) for the month minus the average Darwin MSLP for the month; P_{diffav} is the long term average of P_{diff} for the month; and SD (P_{diff}) is the long term standard deviation of P_{diff} for the month.

While the formula is fairly standard, values are commonly multiplied by 10 to rescale data, resulting in a range from approximately -35 to 35. The SOI is usually computed on a monthly basis for a time period of a year or longer. The values of the index are obtained from the aforementioned sources and the fluctuation of the monthly values is demonstrated in Figure 4. As it is shown in the figure, Nino indices are very similar, while SOI tracks close to these indicators in an inverse form.

3. Pacific Decadal Oscillation (PDO)

PDO index was noted by fisheries scientist Steven Hare in 1996, based on observations of Pacific fisheries cycles and has often been described as a long-lived El Niño-like pattern of Pacific climate variability (Zhang et al. 1997). PDO is based on the monthly sea surface temperature variability of the Pacific Ocean north of 20°N on decadal scale, while the global average anomaly is subtracted from the SSTs to account for global warming (Mantua et al. 1997). Normally, only November to March values are used in calculating the PDO index because year to year fluctuations are most apparent during the winter months (Mantua and Hare, 2002). Even though the PDO and ENSO are related to the same ocean they have two important differences: on one hand 20th century PDO events have a persistence on the order of 20 to 30 years, while, typically ENSO persists for 6 to 18 months. Furthermore, the climate finger prints of the PDO are most visible in the north Pacific while the latter one exists in the tropic. Several studies have indicated two full phases of PDO in the past century (e.g., Mantua

http://dx.doi.org/10.5772/56790

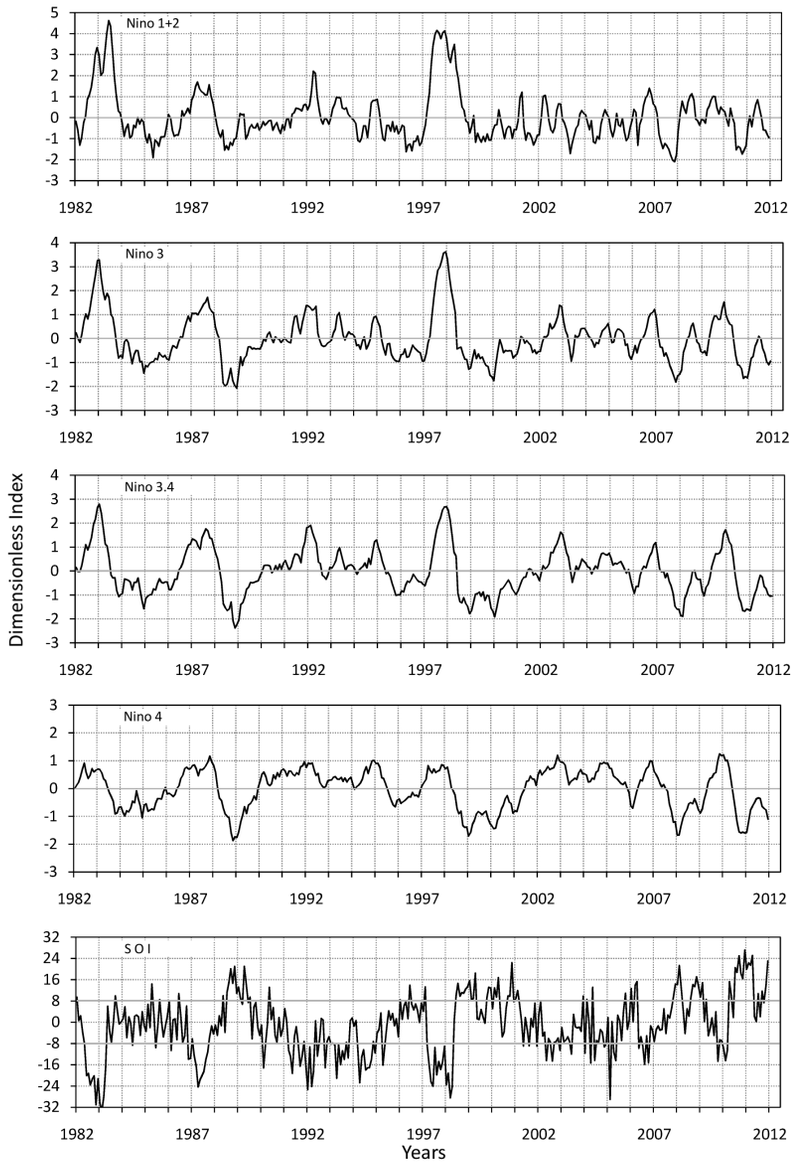

Figure 4. Fluctuation of ENSO indices monthly values during 1982-2011

et al. 1997 and Tootle et al. 2005): cool PDO regimes are reported from 1890-1924 and again from 1947-1976, while warm PDO regimes dominated from 1925-1946 and from 1977 through the mid-1990's. The threshold of cool and warm phases of PDO is zero.

During a positive (warm) phase of PDO the west Pacific is cooler than parts of the eastern Pacific. Opposite pattern occur in the negative or cool phases. These SST fluctuations affect climate patterns of vast regions but the results are more pronounced in the North Pacific. According to precipitation anomalies, positive (warm) phase of the PDO are negatively correlated, mostly, with eastern Australia, Korea, Japan, the Russian Far East and much of Central America (Figure 5) and positively correlated with southwest US. In terms of the temperature anomalies, positive (warm) phase of the PDO tends to coincide generally with anomalously warm temperatures in northwestern North America (r^2>0.16) and cool temper-

atures in eastern China and southeast US (Mantua and Hare, 2002). Pacific salmon production can also be a good indicator of change in PDO phase. Mantua et al. (1997) noted that for much of the past two decades (coincident with the positive PDO phase), salmon fishers in Alaska have prospered while those in the Pacific Northwest have suffered. Yet, in the 1960s and early 1970s, when the Pacific Northwest was under the influence of the negative PDO phase, their fortunes were essentially reversed.

Even in the absence of a comprehensive theoretical or mechanistic understanding, PDO index provides significant predictive information for improving long-term climate forecasts of the regions. This is true because of the PDO's strong tendency for multi-season and multi-year persistence. Gedalofand Smith (2001) applied tree-ring method and Biondi et al. (2001) used ring-widths from moisture stressed trees to reconstruct a PDO index extending back to 1600s. A good source for Monthly values of the index from 1900 to present is the Joint Institute Study of the Atmosphere and Ocean, University of Washington (http://jisao.washington.edu/pdo/). Figure 6 shows how the November-to-March average values for the PDO index have shifted phases and varied over the past decades.

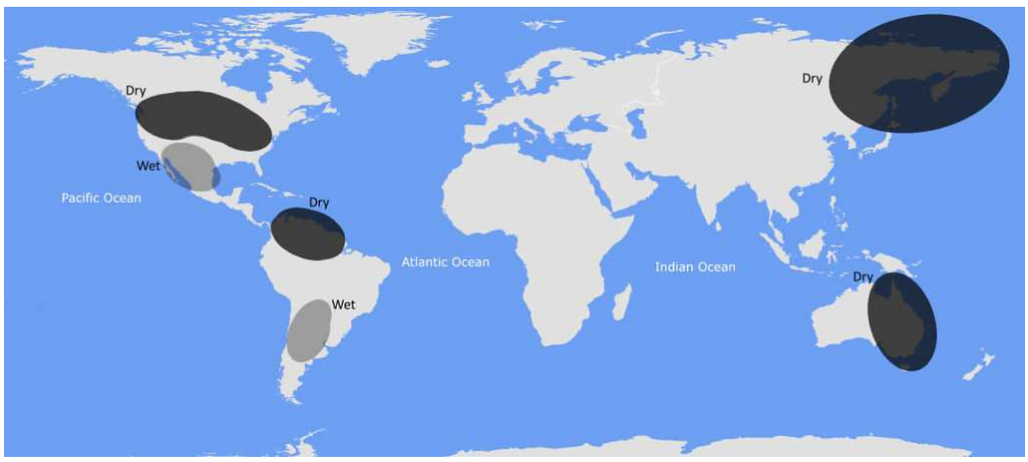

Figure 5. The regions having impacts of PDO

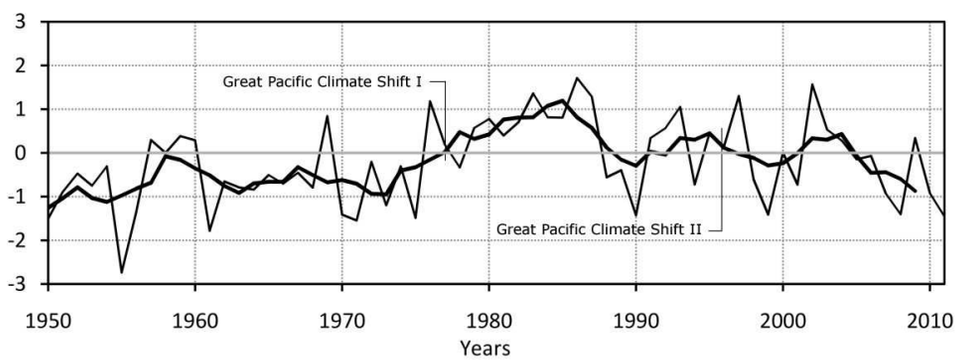

Figure 6. Fluctuation of the Nov-Mar averaged PDO index, with a 5-year running average (bold line).

http://dx.doi.org/10.5772/56790

4. North Atlantic Oscillation index (NAO)

The winter time station-based NAO index is the climate variability mode in North Atlantic Ocean and is defined as the difference in normalized mean winter (December to March) sea level pressure (SLP) anomalies between the *Stykkisholmur/Reykjavik*, Iceland and *Lisbon*, Portugal (Hurrell 1995). But this is not the only acceptable method for defining the index. Most modern NAO indices are based either on the simple difference in surface pressure anomalies between various northern and southern locations as Gibraltar and Reykjavik sites (Jones et al., 1997 and Brandimarte et al., 2011), or on a Principal Component (PC) time series approach (e.g., Portis et al.,2001 and Hurrell and Deser, 2009). The station-based method incorporates the simplicity of data construction into data availability for a period extending back to middle 19th century. A limitation of this approach is that it is unable to track the movement of the NAO centers of action through the annual cycle, owing to the spatial distribution and fixed nature of the station network used. Also, individual station pressure readings can be noisy due to small-scale and transient meteorological phenomena unrelated to the NAO. The PC-based method has the advantage of using gridded sea level pressure data and can be a better representation of the phenomenon according to its dimensions. On the other hand, this approach is limited to the recent decades as the remote sensed SST data became available for every grid of the oceans. More detailed discussions of issues related to the NAO indices are available in Hurrelland Deser (2009) and Hurrell et al. (2003).The threshold of warm and cool phase of NAO signal is zero and each phase might last several years.

NAO affects the strength and tracks of westerly winds and storms across the Atlantic and into Europe (particularly in winter) which in turn results in changes in temperature and precipitation patterns often extending from eastern North America to western and central Europe (Dettinger and Diaz, 2000). Westerly winds blowing across the Atlantic bring moist air into Europe. In NAO positive phases westerly winds are strong and lead to increased rainfall, cool summers and mild and wet winters across northern Europe, below average temperatures and precipitation in Greenland and oftentimes across southern Europe and the Middle East and to a lesser extent warmer winter over eastern North America and eastern South Canada. In contrast, if the index is negative, westerly winds are suppressed, the temperature in central and northern Europe and also southern United States is more extreme in summer and these areas suffer cold winters. Storms track southerly toward the Mediterranean Sea and this brings increased storm activity and rainfall to southern Europe and North Africa. Especially during the months of November to April, the NAO is responsible for much of the variability of weather in the North Atlantic region, affecting wind speed and wind direction changes, changes in temperature and moisture distribution and the intensity, number and track of storms.

The index shows annual variability but has the tendency to remain in single phase for intervals lasting several years (Hurrell 1995). Hurrell and van loon (1995) reported the NAO cool phase from 1952-1972 and 1977-1980 and also warm phases from1950-1951, 1973-1976, and 1981 to present. Winter time (December through March-JDFM), monthly, seasonal and annual NAO values are obtainable from the US National Center for Atmospheric Research (NCAR) (http://www.cgd.ucar.edu/cas/jhurrell/indices.html).The anomalies of the Hurrel station-based and PC-based DJFM NAO indices are demonstrated in Figure 7.As shown in the figure, their

behavior is very close to each other. In station-based method, the SLP anomalies at each station were normalized by dividing each seasonal mean pressure by the long-term mean (1864-1983) standard deviation.

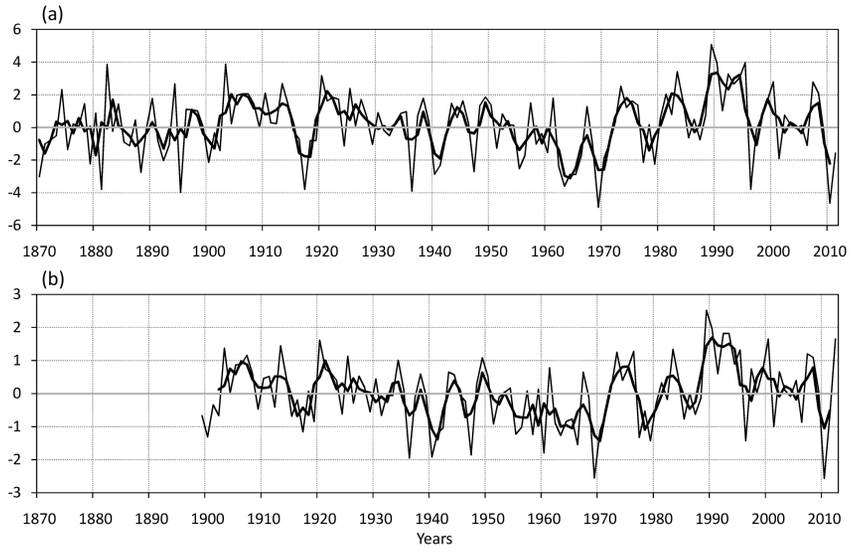

Figure 7. Fluctuation of (a) Hurrell station-based DJFM NAO index and (b) Hurrell PC time series of DJFM SLP over Atlantic sector (20-80°N, 90°W-40°E), with three-year running average (bold line).

5. Atlantic Multi-decadal Oscillation index (AMO)

The continuing sequences of long-duration changes in the de-trended sea surface temperature over the North Atlantic from 0-70°N are termed Atlantic Multi decadal Oscillation (AMO), with cool and warm phases that can last from 20-40 years at a time (Enfield et al. 2001).The time series of the index are calculated from the Kaplan SST dataset which is updated monthly and are created in two versions: smoothed and unsmoothed. The former version is smoothed with a 121 month smoother using earlier 61 and later 60 months values. While the observed AMO cycles are only available at most for the last 150 years, paleo-reconstructed climate data using methods such as tree rings and ice cores have shown that oscillations similar to those observed by instrument have been occurring for approximately the past five centuries (Gray et al., 2004). These large swings in North Atlantic SSTs are probably caused by natural internal variations in the strength of ocean thermohaline circulation and the associated meridional heat transport (Collins and Sinha, 2003). In the 20th century, the climate swings of the AMO have alternately camouflaged and exaggerated the effects of global warming, and have made attribution of global warming more difficult. Threshold of different phases of AMO signal is 0 and each phase lasts between 20 to 40 years.

Recent research has demonstrated that AMO has effects on the regional atmospheric circulation and on associated anomalies in precipitation and surface temperature over much of the Northern hemisphere, in particular, the United States, southern Mexico and probably Western

http://dx.doi.org/10.5772/56790

Europe and Sahel in Africa (Sutton and Hodson, 2005) as shown in Figure 8.Enfield et al. (2001) showed that there is a significant negative correlation with US continental rainfall, with less (more) rain over most of the central USA during a positive (negative) AMO index. According to Zhang and Delworth (2006) warm phase AMO strengthens the summer rainfall in India and Sahel in Africa and the Atlantic Hurricane activity. Apart from the research focusing on time mean anomalies, the index is also associated with changes in the frequency of extreme events. Droughts with broad impacts over the conterminous U.S. (1996, 1999-2002) were associated with North Atlantic warming (positive AMO) and northeastern and tropical Pacific cooling (negative PDO).When the AMO is in its warm phase, these droughts tend to be more frequent and/or severe and opposite occurs in the AMO negative phase (McCabe et al., 2004).

Monthly AMO index values comprising cold (negative) and warm phases (positive index) are accessible from the National Oceanic Atmospheric Administration (NOAA) site (http://www.esrl.noaa.gov/psd/data/timeseries/AMO/).The threshold that separates the phases is the zero line. As shown in Figure 9, warm phases occurred during 1860-1880 and 1930-1960, and cold phases occurred during 1905-1925 and 1970-1990. Since 1995, the AMO has been positive, and it seems the condition has persisted long enough to be considered a new warm phase.

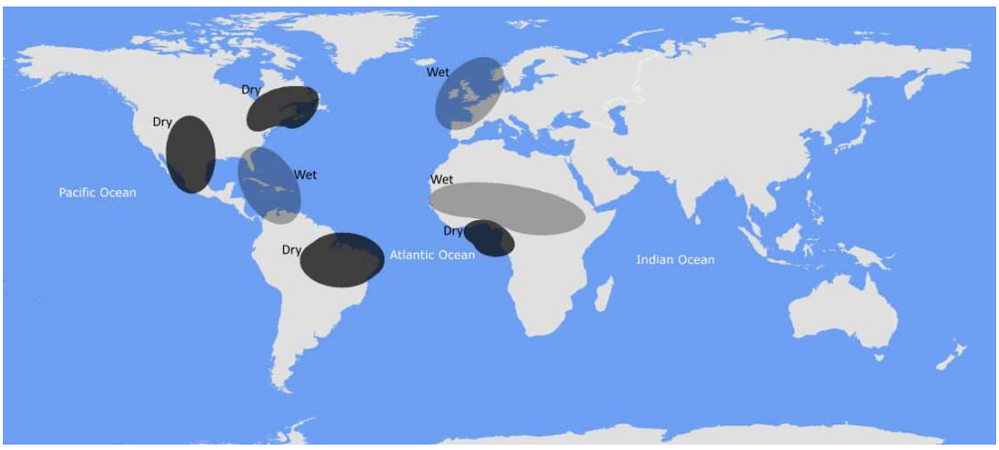

Figure 8. The regions having impacts of AMO

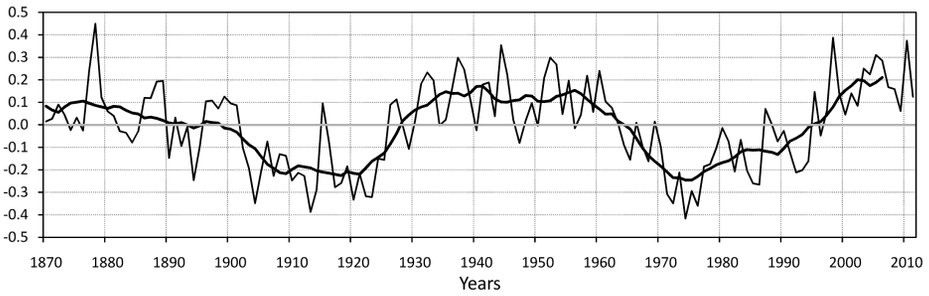

Figure 9. Fluctuation of the AMO index during 1870-2011 with a 10-year running average (bold line). The units on the vertical axes are °C.

6. Inter Tropical Convergence Zone (ITCZ)

ITCZ is the zone where the winds originating in the northern and southern hemispheres converge. In the Northern Hemisphere tropical region, the trade winds move in northeasterly direction, while in the Southern Hemisphere tropics, they are south easterly. Solar heating in the region results in a vertical motion in the air, leading to bands of clouds causing showers and thunderstorms around the equator. Unlike the zones north and south of the equator where the trade winds flow, within the ITCZ the average wind speeds are slight. Early sailors named this belt of calm *the doldrums* because of the inactivity and stagnation they found themselves in after days of no wind.

The location of the ITCZ varies throughout the year (Figure 10) and leads to different wet seasons in many equatorial regions. It also results in the wet and dry seasons in the tropics rather than the four seasons of higher latitudes. Over land, the north-south position follows a meandering path linked to the zenith of the sun, with width of several hundred kilometers, typically reaching a latitude of about 20° north or south, but with effects extending as far as 45° north in parts of southeast Asia. This often leads to two wet seasons and two dry seasons near the equator, merging into a single wet and dry season at the northern and southern limits (Sene, 2010).

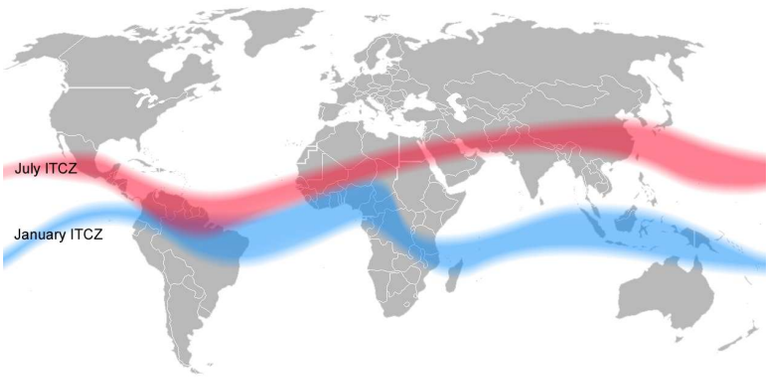

Figure 10. Movement of ITCZ during a year (source: Wikipedia, public domain)

7. Madden Julian Oscillation (MJO)

Scientists have identified many climatic phenomenon that fluctuate on time scales of several years to decades and multi decades, but they are now recognizing atmospheric anomalies on time scales of days to weeks that may influence the evolution of these longer oscillation processes. In 1971 Roland Madden and Paul Julian reported a 40-50 day oscillation when analyzing zonal wind anomalies in the tropical Pacific. This discovery was significant because it was believed until recently that the tropical weather variations on time scales less than one year are essentially random.

http://dx.doi.org/10.5772/56790

The MJO is an intra-seasonal atmospheric variability in the tropics. It is characterized by eastward propagation, moving slowly (~5 m/s) through the atmosphere and over the warm parts of the Indian Ocean into the west and central Pacific. It constantly interacts with the underlying ocean and influences many weather variations as well as lower and upper level wind speed and direction, cloudiness, rainfall, sea surface temperature and ocean surface evaporation (Madden and Julian, 1971; Zhang, 2005). There is a strong year-to-year variability in MJO activity, with periods of strong activity followed by long period in which the Oscillation is weak or absent (Zhang, 2005). In addition to strongly modulating the rainfall in the tropics and to a lesser extent in mid-latitudes; there is evidence that the MJO has effects on other meteorological variables like ENSO and the Indian monsoon. The inter-annual variability of the MJO is partly linked to the ENSO cycle. Strong MJO activity is often observed during weak La Niña years or during ENSO neutral years, while weak or absent MJO activity is typically associated with strong El Niño episodes (Kessler and Kleeman, 2000). Also the Australian, Asian, South American and North American monsoons can all be influenced by the MJO.

The climate prediction center of NOAA maintains an archive of MJO indices from 1978 to present which is accessible at the following address:

(http://www.cpc.ncep.noaa.gov/products/precip/CWlink/daily_mjo_index/mjo_index.html).

8. Sea Surface Temperature (SST) data

Ocean-atmospheric indices like PDO, NAO, AMO and SOI are commonly used as predictors in hydrological forecasting models but for some regions it makes sense to use the SSTs of nearby seas. Studying the coupled local SSTs and hydroclimatic events in regions such as United States (Tootle and Piechota, 2008), Colombia (Tootle et al., 2008), Brazil (Uvo et al., 1998) and Sri Lanka (Chandimala and Zubair, 2007) has assisted the identification of regions that are not represented in the existing series of Pacific, Atlantic and Indian Oceans SSTs. The mentioned studies resulted in greater correlation values than those of well-known climatic indices. Therefore, local experiments are highly recommended for evaluating effective regions of the seas in correlation with hydrological responses of local areas. For example for a country like Iran as well as several others in the Middle East two optimal candidates could be Mediterranean and Persian Gulf's sea surface temperatures. NOAA_OI_SST_V2 data provided by the NOAA/OAR/ESRL PSD, obtained from their Web site (http://www.esrl.noaa.gov/psd) are used as Mediterranean and Persian Gulf's SSTs. Reynolds et al. (2001) used *in situ* data observed from many ships, buoys and AVHRR satellite data, and utilized some modification methods. Reynolds Optimum Interpolation (OI.V2) monthly and weekly SST data are available from November 1981 to present for 1° grid squares of the seas.

8.1. Persian Gulf SST

The Persian Gulf, having a vast amount of crude oil and natural gas reserves of earth, is an important economic, military and political region. The shallowness of the Gulf (average depth ~36 m), the high evaporation rate, combined with a limited exchange through the Strait of

Hormuz cause the formation of a salty and dense water mass called Persian Gulf Water (PGW), which is apparently the warmest sea in the world with temperature reaching 35.6°C in the summer. The Persian Gulf is almost 990 km long extending from *Shatt-Al-Arab* (also called *Arvand-Roud*) as a major river source located at the head of the Gulf, which is fed by Euphrates, Tigris and Karoun rivers, to the Strait of *Hormuz* where it connects to the Oman Sea. It has a maximum width of 370 km with a surface area of about 239,000 km^2 (Emery, 1956). Extensive shallow regions (<20m) also occur along the coast of United-Arab-Emirates and Bahrain and Deep portions (>40m) are found along the Iranian coast continuing to the Oman sea (Kämpf and Sadrinasab, 2006).

The Strait of *Hormuz* acts as an exchange point between the Persian Gulf and Indian Ocean. The characteristic of the in/out flow at the strait has been investigated by many studies (e.g., Bower et al., 2000; John et al., 2003; Pous et al., 2004).At the head of the Oman Sea, where the Persian Gulf connects to Global Oceans, the fresher and colder inflow of Indian Ocean surface water (IOSW) core is clearly seen above and next to the Persian Gulf water outflow (Pous et al., 2004). In a research by John et al. (2003), the moored time series records show a relatively steady deep outflow through the strait from 40 m to the bottom with a mean speed of approximately 20 cm/s. A variable flow is found in the upper layer with frequent reversals on timescales of several days to weeks. The annual mean flow in the near-surface layer is found to be northeastward (out of the Persian Gulf) in the southern part of the strait, suggesting a mean horizontal exchange with the Indian Ocean that is superimposed on the vertical overturning exchange driven by evaporation over the gulf. Bower et al. (2000) studied the seasonal variability of the formation of dense PGW outflow and the surrounding oceanic environment with temperature and salinity profiles and found that the outflow salinity is slightly lower in winter (~0.5 practical salinity unit) than in summer and the temperature is cooler by about 3°C in winter.

Prevailing winds over the Persian Gulf are northwesterly. During winter (November-February) the winds are slightly stronger (~5 m/s) than those during the summer (June-September) (~3 m/s). The best known phenomenon in the Persian Gulf that can cause abrupt changes in the circulation and heat-budget for a short period of time is *shamal*, a northwesterly wind occurring during winter as well as summer (Perrone, 1979). Based on duration, there are two types of winter *shamal*: those which last 24-36 hours and those which last for a longer period of 3 to 5 days. The winds bring cold dry air (T=20°C) and result in SST cooling of about 10°C noticeably in the northern and shallower shelf regions (Thoppil and Hogan, 2010). The other air masses affecting the area, mostly in winter, is Sudan current. About 30% of the total rain-bearing air masses coming to Iran originate in North Africa, Red Sea and Saudi Arabia which is called Sudan current (Khalili, 1992) (Figure11).

The general water circulation of the Persian Gulf is cyclonic, which is bounded by an Iranian Coastal Current (ICC) flowing northwestward along the northern side from the Strait of *Hormuz* with speed greater than 10cm/s, and a southeastward current in the southern part of the Gulf. The ICC, which flows against the prevailing northwesterly winds, is primarily driven by the pressure gradient. The dense bottom outflow forming in the southern shallows flows along the coastline of UAE (Hunter, 1983; Reynolds, 1993).

http://dx.doi.org/10.5772/56790

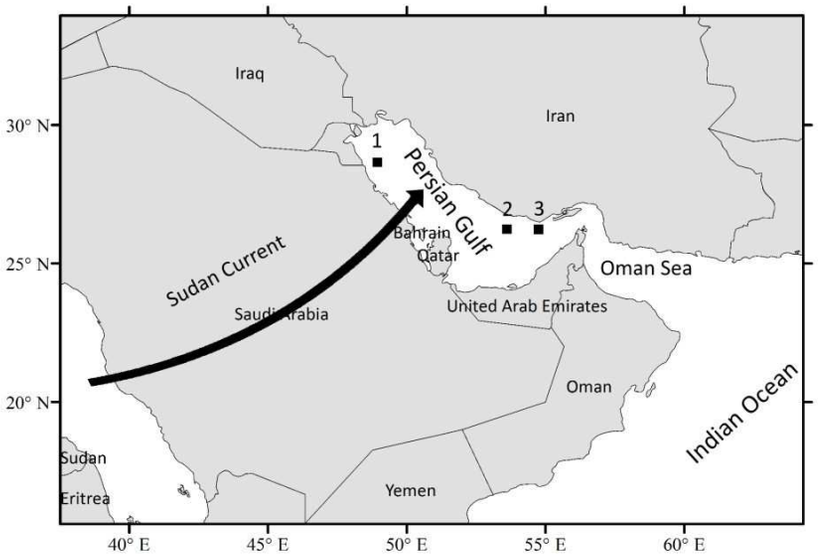

Figure 11. Persian Gulf location and general track of air masses toward Iran during winter

The Persian Gulf SSTs could be used as possible predictors of hydrological parameters for countries around it, including Iran. It has been shown (Nazemosadat, 1998)that winter droughts and wet periods of South western Iran tend to coincide with periods when the Persian Gulf SSTs are above (below) normal. Overall, correlation analysis between rainfall and SST data, using various data lengths, has revealed that the fluctuations of SST account for about 40% of rainfall variability over the region.

Using OI.V2 data, the anomalies of monthly SST values for three selected points shown in Figure11 are demonstrated as an example in Figure 12. It is shown that the eastern parts are possibly warmer than northwestern ones. Besides, a warming trend is noted for all points by applying a trend line for the annual mean values (dotted line). For example, the mean annual warming rate for point 2 is calculated at 0.035°C/year which should be considered in long-term forecasting. A noteworthy point, that needs more analysis, is the similar fluctuation of annual values in all three diagrams showing a possible change phase every 2 to 4 year.

8.2. Mediterranean SST

The Mediterranean Sea is located in the middle of the Mediterranean. The main rainy season over the Mediterranean Sea extends from October to March, but maximum rainfall occurs during November-December. During the rainy season western Mediterranean Sea receives ~20% larger rainfall compared to eastern Mediterranean Sea (Mehta and Yang, 2008). Mediterranean Sea has climatic dynamics that affect the climate of various areas around, including Sahel in Africa (Rowell, 2003), Turkey (Kutiel, 2001), Iran (Araghinejad and Meidani, 2012), and Greece (Kassomenos and McGregor, 2006). Due to its size and limited exchange at Gibraltar Strait, Mediterranean Sea dynamics is mainly linked to the local climate and it is particularly sensitive to anthropogenic climatic perturbations (Skiliris et al., 2011). Several studies (e.g. Rixen, 2005; Belkin, 2009) have demonstrated the rapid surface warming of the sea during the last decades that should be considered in long-lead forecasting when these SSTs

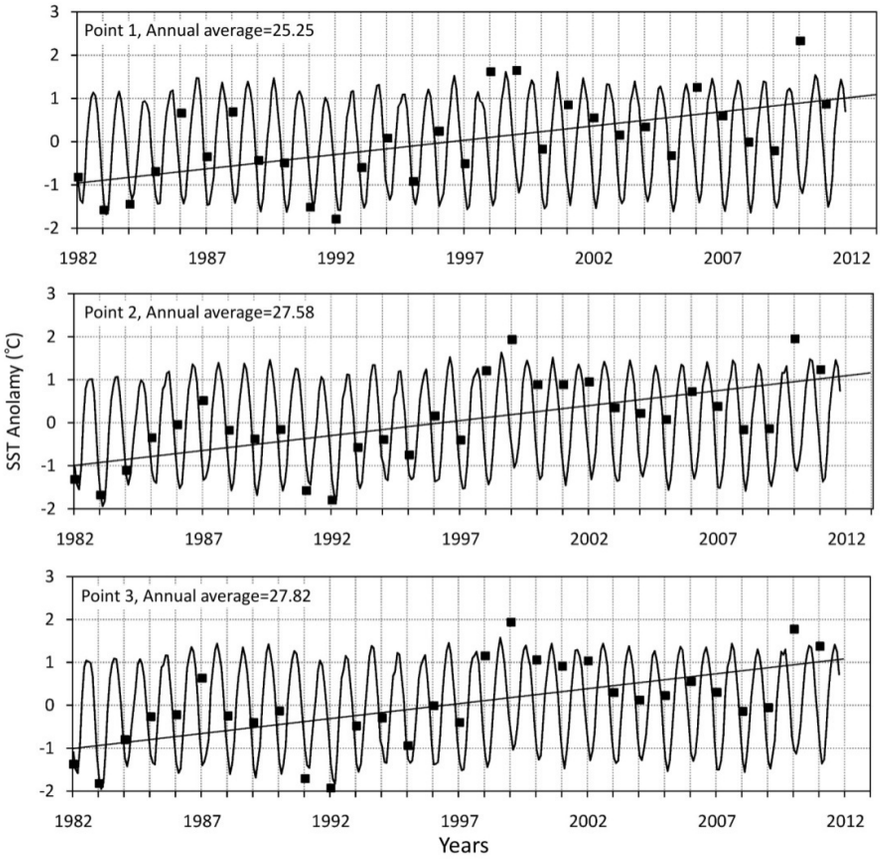

Figure 12. Fluctuations of Persian Gulf SSTs for selected points during 1982-2011.

are used as predictors. Skilirish (2011) reported the satellite-derived mean annual warming rate of about 0.037°C/year for the whole basin, about 0.026°C/year for the western sub-basin and about 0.042°C/year for the eastern sub-basin over 1985-2008.

During the northern hemisphere winter, the high pressure cells over the north Atlantic are centered at about 30°N and those over Asia at about 45°N. Between them lies the Mediterranean region, an area of warm and moist air, with a tendency for low pressure. So along the north coast of Africa all the way from Morocco to Egypt, the prevailing winds in winter are westerly, controlled by the low pressure over the Mediterranean. During the northern summer the subtropical high pressure cells of the northern hemisphere are found in well-marked anti cyclone over the oceans. The Asia and Africa continents are relatively hot, the air over them expands, and a low pressure system results, changing the prevailing winds direction from north to south and southwest (Kendrew 1922). As shown in Figure 13, the Mediterranean currents influence mostly west and, to a lesser extent, the center of Iran in winter.

Rezaebanafsheh (2011) studied the relationship between winter and autumn precipitation with previous season anomalies of Mediterranean SST at several stations in western Iran and showed that the cooler condition of the sea in autumn leads to wetter winter in the study area, but the correlation of the summer SST anomalies with autumn precipitation was not significant.

http://dx.doi.org/10.5772/56790

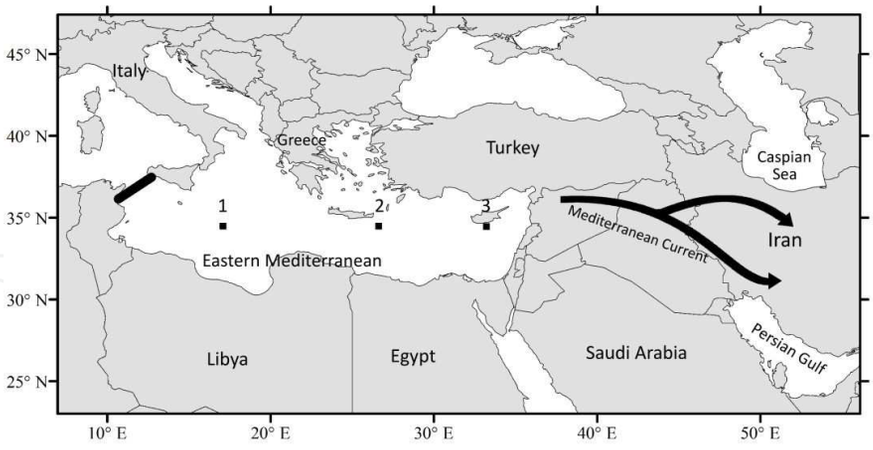

Figure 13. Mediterranean Sea location and general track of air masses toward Iran during winter

Rainfall amounts differ markedly from place to place over the Mediterranean. Sea surface temperatures are highest in the eastern Mediterranean compared to elsewhere in the sea. Fluctuation of standard values of average monthly SSTs over the Mediterranean Sea, using OI.V2 data are shown in Figure 14. Apart from the warming rate mentioned in the literature, similar to Persian Gulf, the annual values of the SSTs (dotted line) show a shift in phase every 2 to 4 year.

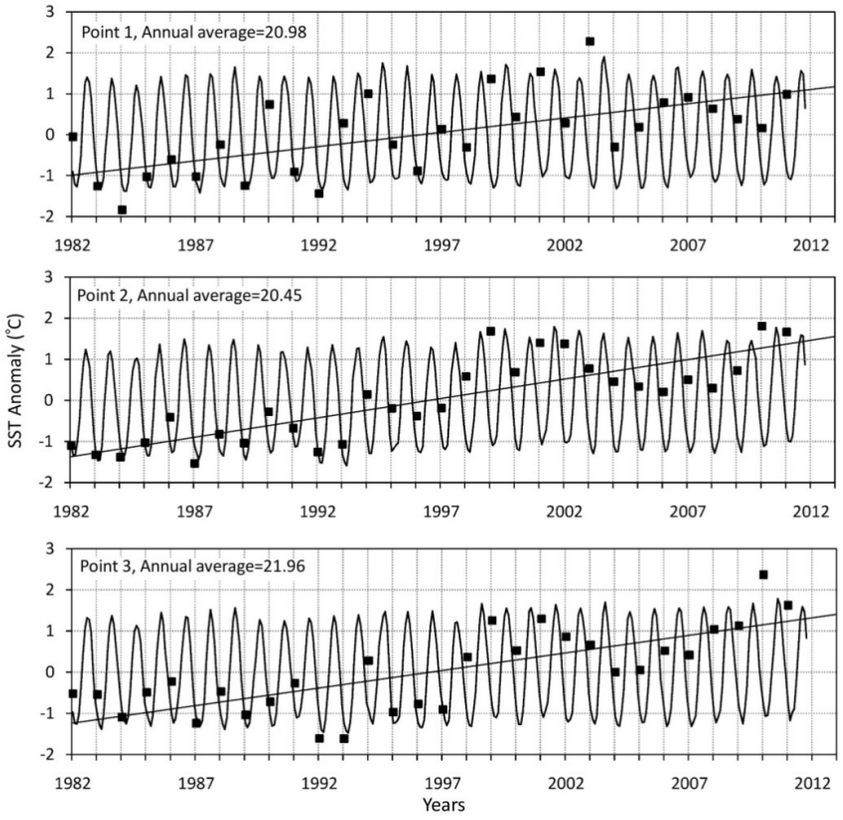

Figure 14. Fluctuations of Mediterranean SSTs for selected points during 1982-2011

9. The effects of large scale climate signals around the world

The effects of large scale climate signals on different locations of the world need to be studied and investigated in order to identify the specific dominant signals that impact each region. As mentioned previously, such background information provides useful context for assessing pattern changes due to climate change. The results could also be used for long-lead hydroclimatic forecasts. Tables 2 to 5 are selected compilation of various teleconnections and their hydro-climatological impacts around the world as documented in easily accessible literature.

The table shows researchers, the location of the study, the preferred climate signals as predictors, an overview of the paper as well as the time period that the study was conducted.

Reference	Location	Time period*	Preferred Climatic predictors	Overview
Ropelewski and Halpert, 1987	Eastern Africa	Various time periods	ENSO	During the LaNina event, the eastern Ecuadorian Africa experiences more than normal rainfall meanwhile the eastern sought of Africa experiences less than normal rainfall
Nicholson and Kim, 1997	Africa	1901-1990	ENSO	La Nina and El Nino cause wet and dry years, respectively. However the type of impacts of El Nino has a more variation in different time and locations
Nicholson and Selato, 2000	Africa	1901-1990	ENSO	They obtained the same results as Ropelewski and Halpert, (1987) by studying a wider region
Rowell, 2003	Sahel in Africa	1947-1996	Mediterranean SSTs	Warmer than average Mediterranean leads to a wetter than normal Sahel

* Time period covered in the study

Table 2. A select list of studies showing locations in Africa where teleconnection indices are related to hydrological parameters

Reference	Location	Time period	Preferred Climatic predictors	Overview
Schonher and Nicholson, 1989	California	1950-1980	ENSO	There is a relationship between ENSO and wet years
Mantua et al., 1997	North America	1900-1996	PDO	During warm PDO years, wintertime precipitation decreases over much of the interior of North America and Alaskan salmon catches increases
Uvo et al., 1998	Northeast Brazil	1946-1985	Pacific and Atlantic SSTs	During April-May, North tropical (neg) and South tropical Atlantics (pos) and equatorial pacific (neg) are most correlated regions

http://dx.doi.org/10.5772/56790

Reference	Location	Time period	Preferred Climatic predictors	Overview
Jones, 2000	The U.S. (California state)	1958-1996	MJO	Slightly more extreme rainfall occur as convective anomalies are located over the Indian Ocean
Enfield et al., 2001	United States	1856-1999	AMO	AMO warmings decrease annual rainfall over U.S., especially over the eastern Mississippi basin
Karla and Ahmad, 2009	Western United States	1906-2001	ENSO and NAO	ENSO and NAO are better predictors for long-lead Streamflow forecasting of Upper Colorado River Basin as compared to PDO and AMO
Kayano and Sansigolo, 2009	Southern Brazil	1913-2006	ENSO (Nino 3.4), SSTs of southwestern subtropical Atlantic	Excessive rainfall during El-Niño and higher TMIN by warming of SSA ocean surface water
Barrett et al., 2012	Chile	1980-2010	MJO	Positive precipitation anomalies in central and south-central Chile for MJO phases 8, 1 and 2, and negative anomalies in phases 3-7
Tootle and Piechota, 2006	United States	1951-2002	North central and near the tropical Pacific, northern South American coast and northern Atlantic Ocean are most correlated regions, considering all years	PDO, ENSO and AMO were acknowledged as effective regions on the continental US streamflow variability
Tootle et al., 2008	Colombia	1960-2000	Eastern coast of Australia, Equatorial and South central Pacific SSTs as most correlated regions	An El-Niño (La-Niña) will result in decreased (increased) streamflow
Karla and Ahmad, 2009	Western United States	1906-2001	ENSO and NAO	ENSO and NAO are better predictors for long-lead Streamflow forecasting of Upper Colorado River Basin as compared to PDO and AMO
Kayano and Sansigolo, 2009	Southern Brazil	1913-2006	ENSO (Nino 3.4), SSTs of southwestern subtropical Atlantic	Excessive rainfall during El-Niño and higher TMIN by warming of SSA ocean surface water
Barrett et al., 2012	Chile	1980-2010	MJO	Positive precipitation anomalies in central and south-central Chile for MJO phases 8, 1

Reference	Location	Time period	Preferred Climatic predictors	Overview
				and 2, and negative anomalies in phases 3-7

* Time period covered in the study

Table 3. A select list of studies showing locations in America where teleconnection indices are related to hydrological parameters

Reference	Location	Time period	Preferred Climatic predictors	Overview
Nazemosadat, 1998	Southern Iran	1951-1987	Persian Gulf SSTs	Winter droughts and wet periods tend to occur when PGSSTs are above and below normal, respectively
Kutiel et al., 2001	Eastern Mediterranean region over Turkey	1929-1996	Sea Level Pressure (SLP)	Positive SLP departures are associated with dry conditions of Turkey and vice versa. The relationship is large in winter
Wheeler and Hendon, 2004	Australia and India	1979-2001	MJO	Monsoons occur mostly during the enhanced half of the MJO cycle and rarely during the suppressed half. In Darwin, Australia, the likelihood of extreme rainfall becomes triple from dry to wet phase of MJO
Power et al., 2005	Australia	Over 100 years	ENSO	In general, El-Niño events are associated with drying and la-Niña events with increased rainfall, but, asymmetrically.
Araghinejad et al., 2006	Iran, Isfahan	1969-2001	SOI, NAO and Snow Budget	Higher SOI values (Jan-Oct) corresponds to drier autumn and winter seasons and higher NAO values corresponds to wetter spring
Sen Roy, 2006	India and eastern Arabian Sea	1925-1998	ENSO and PDO	There is negative relationship between Winter precipitation and both ENSO and PDO indices
Chandimala and Zubair, 2007	Sri Lanka	1950-2000	ENSO, and Indian Ocean SSTs	Reduced streamflow (Apr-Sep) and enhanced rainfall (Oct-Dec) during El-Niño are dominant
Zhang et al., 2009	Southeast China	1980-2010	MJO	The perceptible water decreases on intraseasonal time scales as the

http://dx.doi.org/10.5772/56790

Reference	Location	Time period	Preferred Climatic predictors	Overview
				convective center moves from the Indian Ocean to the western Pacific Ocean
Zhu et al., 2010	East China	1951-2008	PDO	The shift of the PDO to a negative phase increases rainfall in the Huang-Huai river region and decreases in the Yangtze river region

* Time period covered in the study

Table 4. A select list of studies showing locations in Asia and Australia where teleconnection indices are related to hydrological parameters

Reference	Location	Time period	Preferred Climatic predictors	Overview
Feudale and Shukla, 2007	Europe	2003	Mediterranean SSTs	The SSTs are able to simulate the upper level anticyclone over central Europe, but to a lesser extent than global SST.
Hurrel et al., 2003	North America, North Africa, Europe and Middle East	-	NAO	During NAO positive phase, much of central and southern Europe, Mediterranean and Middle East are drier, eastern U.S. and Iceland through Scandinavia are wetter, North Africa and Middle East are cooler and North America is warmer
Sutton and Hodson, 2005	The U.S., Europe and Sahel in Africa	1931-1990	AMO	AMO warm phase cause decreased summer precipitation and warmer temperature in the U.S., increased precipitation in Europe and Sahel and warmer temperature in western Europe
Zhang and Delworth, 2006	India and Sahel in Africa	1901-2000	AMO	AMO, with a positive correlation, play a leading role in the 20th century multidecadal variation of India/Sahel summer rainfall and Atlantic Hurricane activity
Brandimarte et al., 2011	Mediterranean Areas (southern Italy and Nile Delta in Egypt)	1920-1996	NAO	Hydroclimatic variables of most of the Mediterranean areas are negatively correlated with NAO, while southeastern parts have a weaker positive correlation

* Time period covered in the study

Table 5. A select list of studies showing locations in Europe and multi-continents where teleconnection indices are related to hydrological parameters

10. Summary

The chapter reviewed the status of knowledge concerning teleconnection ocean-atmospheric dynamics. Different climate signals such as Southern Oscillation (SO), Pacific Decadal Oscillation (PDO), North Atlantic oscillation (NAO), Atlantic Multi-decadal Oscillation index (AMO), Madden Julian Oscillation (MJO), Inter Tropical Convergence Zone (ITCZ), and Sea Surface Temperature (SSTs) of two large scale water bodies were reviewed. In addition to providing basic information, the reports on the effect of those signals in different regions of the world were reviewed in terms of their potential as long-lead hydroclimatological predictors of rainfall. The effects of climatic signals on different regions were reviewed based on the recent studies of different researchers and scientists. The information provided is useful for assessing probable changes in the frequency and magnitude of these teleconnection indices as a result of climate change.

Author details

Shahab Araghinejad and Ehsan Meidani

College of Agricultural Technology and Science, University of Tehran, Karaj, Iran

References

[1] Araghinejad, S., Burn, D.H., and Karamouz, M. (2006). "Long-lead probabilistic forecasting of streamflow using ocean-atmospheric and hydrological predictors." Water Resour. Res., Vol. 42, DOI: 10.1029/2004WR003853.

[2] Araghinejad, S., Meidani, E. (2012). "Probabilistic Drought Forecasting for a Basin Scale Water Resources Operation." HydroPredict2012 conference, Vienna, Austria, 24-27 Sep.

[3] Barrett, B., Carrasco, J.F., Testino, A.P. (2012). "Madden–Julian Oscillation (MJO) Modulation of Atmospheric Circulation and Chilean Winter Precipitation." J. Clim., Vol. 25, pp 1678-1688. DOI:10.1175/JCLI-D-11-00216.1

[4] Beebee, R.A., and Manga, M. (2004). "Variation in the relationship between snowmelt runoff in Oregon and ENSO and PDO." J. Am. Water Resour. Assoc., 40(4), 1011–1024, DOI:10.1111/j.1752-1688.2004.tb01063.x.

[5] Belkin, M. (2009). "Rapid warming of large marine ecosystems." Progr. Oceanogr., 81, 207–213.

[6] Biondi, F., Gershunov A., and Cayan D.R., (2001): North Pacific decadal climate variability since 1661. J. Climate, 14, 5–10.

[7] Bower, A.S., Hunt H.D., and Price J.F. (2000). "Character and dynamics of the Red Sea and Persian Gulf outflows." J. Geophys. Res., 105(C3), pp 6387-6414.

[8] Brandimarte, L., Baldassarre, G.D., Bruni, G., D'Odorico, P., Montanari, A., (2011). "Relation between the North-Atlantic Oscillation and Hydroclimatic Conditions in Mediterranean Areas." Water Resour Manage, Vol. 25, pp 1269–1279. DOI 10.1007/s11269-010-9742-5.

[9] Chandimala, J., Zubair, L. (2007). "Predictability of stream flow and rainfall based on ENSO for water resources management in Sri Lanka." J. Hydrol. Vol. 335, pp 303–312

[10] Collins, M., and Sinha, B. (2003). "Predictability of decadal variations in the thermohaline circulation and climate." Geophy. Rese. Let. Vol. 30, NO. 6, 1306, DOI: 10.1029/2002GL016504

[11] Dettinger, M.D., and Diaz, H.F. (2000). "Global Characteristics of Streamflow Seasonality and Variability." J. Hydrometeorology, Vol. 1, pp 289-310

[12] Enfield, D.B., Mestas-Nunez, A.M., and Trimble, P.J. (2001). "The Atlantic Multidecadal Oscillation and its relation to rainfall and river flows in the continental U.S." Geophy. Rese. Let., Vol. 28, No.10, pp 2077-2080.

[13] Emery, K O.1956. "Sedimentsand and waters of Persian Gulf", Bull. Amer. Assoc.

[14] Feudale, L., and Shukla, J., (2007). "Role of Mediterranean SST in enhancing the European heat wave of summer 2003." Geophy. Rese. Let., Vol. 34, DOI: 10.1029/2006GL027991.

[15] Gedalof, Z., and Smith D.J., (2001): Interdecadal climate variability and regime-scale shifts in Pacific North America. Geophys. Res. Lett., 28, 1515–1518.

[16] Gray, S.T., Graumlich, J.L., and Pederson, G.T. (2004). "Atree-ring based reconstruction of the Atlantic Multidecadal Oscillation since 1567 A.D." Geophys. Res. Lett., 31, DOI:10.1029/ 2004GL019932.

[17] Hunter, J.R. (1983). "Aspects of the dynamics of the residual circulation of the Arabian Gulf, in: Coastal oceanography." edited by: Gade, H. G., Edwards, A., and Svendsen, H., Plenum Press, 31– 42.

[18] Hurrell, J.W. (1995). "Decadal trends in the North Atlantic Oscillation: Regional temperatures and precipitation." Science, 269(5224), pp 676– 679, DOI:10.1126/science. 269.5224.676.

[19] Hurrell, J.W., and vanLoon, H., (1995). "Decadal Variation in climate associated with the North Atlantic Oscillation." Climate Change, No. 31, pp 301-326.

[20] Hurrell, J.W., and Deser, C. (2009). "North Atlantic climate variability: The role of the North Atlantic Oscillation." J. Mar. Syst., Vol. 78, No. 1, pp 28-41

[21] Hurrell, J.W., Kushnir, Y., Ottersen, G. (2003). "An overview of the North Atlantic oscillation." In: Hurrell, J.W, Kushnir, Y., Ottersen, G., Visbeck, M., (eds) The North Atlantic Oscillation: Climatic Significance and Environmental Impact. American Geophysical Union, pp 1-35.

[22] Johns W.E., F. Yao, D.B. Olson, S.A. Josey, J.P. Grist and D.A. Smeed, 2003, "Observations of seasonal exchange through the Straits of Hormuz and the inferred heat and freshwater budgets of the Persian Gulf." J. Geophys. Res., 108, C12, 3391, doi: 10.1029/2003JC001881.

[23] Jones, C. (2000). "Occurrence of Extreme Precipitation Events in California and Relationships with the Madden–Julian Oscillation." J. Clim., Vol. 13, pp 3576-3587.

[24] Jones, P.D., Jonsson, T., Wheeler, D. (1997). "Extension to the North Atlantic Oscillation using early instrumental pressure observations from Gibraltar and south-west Iceland." Int. J. Climatol. Vol. 17, pp 1433–1450.

[25] Kämpf, J., Sadrinasab, M. (2006). "The circulation of the Persian Gulf: a numerical study." Ocean Science Disc., Vol. 2, pp 1-15.

[26] Karla, A., Ahmad, S., (2009). "Using ocean atmospheric oscillation for long lead time streamflowforcasting". WaterResour. Res., Vol. 45, DOI:10.1029/2008WR006855.

[27] Kassomenos, P.A., and McGregor, G.R. (2006). "The Interannual Variability and Trend of Precipitable Water over Southern Greece." J. Hydromet., Vol. 7, pp 271-284.

[28] Kayano, M.T., Sansígolo, C. (2009). "Interannual to decadal variations of precipitation and daily maximum and daily minimum temperatures in southern Brazil." Theor. Appl. Climatol., Vol. 97, pp 81–90, DOI:10.1007/s00704-008-0050-4

[29] Kendrew, W.G. (1922). "The Climates of the Continents." Oxford University Press.

[30] Kessler, W., and Kleeman, R., (2000). "Rectification of the Madden-Julian Oscillation into the ENSO." cycle. J. Climate, Vol. 13, pp 3560-3575.

[31] Khalili, A. (1992). "Fundamental Study of Iranian Water Resources, Climatological Understanding of Iran, Parts 1 and 2." Jamab consultant reports, the Iranian Ministry of Energy (in Persian).

[32] Kutiel, H., Hirsch-Eshkol, T. R., and Turkes, M. (2001). "Sea level pressure patterns associated with dry or wet monthly rainfall conditions in Turkey." Theor. Appl. Climatol., Vol. 69, pp 39-67.

[33] Madden, R.A., and Julian, P.R. (1971). "Detection of a 40-50-day oscillation in the zonal wind in the tropical Pacific." J. Atmos. Sci., Vol. 28, pp 702–708.

[34] Mantua, N. J., and Hare, S. R. (2002). "The Pacific decadal oscillation." J. Oceanogr., Vol. 58, pp 35–44.

[35] Mantua, N.J., Hare, S.R., Zhang, Y., Wallace, J.M., Francis, R.C. (1997). "A Pacific interdecadal climate oscillation with impacts on salmon production." Bulletin of the American Meteorological Society, Vol. 78, pp 1069-1079.

[36] McCabe, G.J., Palecki, M.A., Betancourt, J.L. (2004). "Pacific and Atlantic Ocean influences on multidecadal drought frequency in the United States." Nat. Acad. Sci. U.S.A., volume 101, 4136-4141

[37] Mehta A.V. and Yang, S., 2008: Precipitation Climatology over Mediterranean Basin from TRMM, Advances in Geosciences, 17, 87-91.

[38] Nazemosadat, M.J. (1998). "The Persian Gulf sea surface temperature as a drought diagnostic for southern parts of Iran." Drought News Network, Vol. 10, pp 12-14.

[39] Nicholson S. E. and Kim J., "The relationship of the El Nino-Southern Oscillation to African rainfall" International Journal of Climatology. Vol. 17, 1997. pp. 117 – 135

[40] Nicholson, S. E. and Selato, J. C., "The influence of LaNina on African rainfall", Int. J. of Climatology, Vol. 20, 2000. pp. 1761-1776

[41] Perrone, T.J. (1979). "Winter shamal in the Persian Gulf." Naval Env. Prediction Res. Facility. Technical Report. 79-06. Monterey, 180pp.

[42] Portis, D.H., Walsh, J.E., El Hamly, M., Lamb, P.J. (2001). "Seasonality of the North Atlantic Oscillation." J. Climate., Vol. 14, pp 2069–2078.

[43] Pous, S.P., Carton, X., Lazure, P. (2004). "Hydrology and circulation in the Strait of Hormuz and the Gulf of Oman—Results from the GOGP99 Experiment: 1. Strait of Hormuz." J. Geophy. Rese., Vol. 109; PART 12; SECT 3; pp. C12037.

[44] Power, S., Haylock, M., Colman, R., Wang, X., 2005. Asymmetry in the Australian response to ENSO and the predictability of interdecadal change sin ENSO teleconnections. Bureau of Meteorology Research Centre. BMRC Report No. 113, 33pp.

[45] Reynolds, R.M. (1993). "Physical oceanography of the Gulf, Strait of Hormuz, and the Gulf of Oman – Results from the Mt Mitchell expedition." Mar. Pollution Bull., Vol. 27, pp 35–59.

[46] Reynolds, R.W., Rayner, N.A., Smith, T.M., Stokes, D.C., and Wang, W. (2001). "An Improved In Situ and Satellite SST Analysis for Climate." Science Applications International Corporaton, Camp Spring, Maryland.

[47] Rezaebanafsheh, M., Jahanbakhsh, S., Bayati, M. and Zeynali, B. (2011). "Forecasting autumn and winter precipitation of west of Iran applying Mediterranean SSTs in summer and autumn." Phy. Geog. Research Quarterly, Vol. 74, pp 47-62.

[48] Rixen, M. (2005). "The Western Mediterranean deep water: a proxy for climate change." Geophys Res. Lett., DOI:10.1029/2005GL022702.

[49] Ropelewski, C.F. and M.S. Halpert, "Global and regional scale precipitation patterns associated with the El Niño/Southern Oscillation". Mon. Wea. Rev., Vol. 115, 1987. pp. 1606-1626.

[50] Rowell, D.P. (2003). "The Impact of Mediterranean SSTs on the Sahelian Rainfall Seasonal." J. Clim., Vol. 16, 5, 849–862.

[51] Schonher, T., and S. E., Nicholson, "The relationship between California rainfall and ENSO events", J of Climate, Vol. 2, 1989. pp. 1258-1269

[52] Sene, K. (2010). "Hydro-meteorology forecasting and applications." Springer, DOI: 10.1007/978-90-481-3403-8

[53] Sen Roy, S., (2006). "The Impacts of ENSO, PDO and local SSTs on winter precipitation in India." Physical Geography, Vol. 27, 5, pp 464-474.

[54] Skiliris, N., Sofianos, S., Gkanasos, A., Mantiziafo, A., Vervatis, V., Axaopoulos, P., and Lascaratos, A. (2011). "Decadal scale variability of sea surface temperature in the Mediterranean Sea in relation to atmospheric vriability." Ocean Dyn., DOI: 10.1007/s10236-011-0493-5.

[55] Sutton, R.T., and Hodson, D.L.R. (2005). "Atlantic Ocean forcing of North American and European summer climate." Science, 309, 115–118.

[56] Thoppil, P.G., Hogan, P.J. (2010). "Persian Gulf response to a wintertime shamal wind event." Deep-Sea Research, 1, 57, pp 946-955, DOI: 10.1016/j.dsr.2010.03.002.

[57] Tootle, G.A., Piechota, T.C. (2006). "Relationships between Pacific and Atlantic ocean sea surface temperatures and US streamflow variability." Water Resources Research, 42, W07411.

[58] Tootle, G.A., Piechota, T.C., Gutierrez, F. (2008). "The relationships between pacific and Atlantic ocean sea surface temperatures and Colombian streamflow variability." J. Hydrol., 349, 268–276.

[59] Uvo, C.B., Repelli, C.A., Zebiak, S.E. and Kushnir, Y. (1998). "The relationships between tropical Pacific and Atlantic SST and northeast Brazil monthly precipitation." J. Clim., Vol. 11, pp 551–562.

[60] Wheeler, M.C., and Hendon, H.H. (2004). "An All-Season Real-Time Multivariate MJO Index: Development of an Index for Monitoring and Prediction." Monthly Weather Review, Vol. 132, pp 1917-1932.

[61] Zhang, C., (2005). "Madden-Julian Oscillation." Rev. Geophys., Vol. 43, DOI: 10.1029/2004RG000158.

[62] Zhang, R., Delworth, T.L. (2006). "Impact of Atlantic multidecadal oscillations on India/Sahel rainfall and Atlantic hurricanes." Geoph. Res. Let., Vol. 33, DOI: 10.1029/2006GL026267.

[63] Zhang, Y., Wallace J.M., Battisti, D.S (1997). "ENSO-like interdecadal variability: 1900-93." J. Clim., Vol. 10, pp 1004-1020.

[64] Zhang, l., Wang, B., Zeng, Q.(2009). "Impact of the Madden–Julian Oscillation on Summer Rainfall in Southeast China." J. Clim., Vol. 22, pp 201-216, DOI: 10.1175/2008JCLI1959.1

[65] Zhu, Y., Wang, H., Zhou, W., Ma, J. (2010). "Recent changes in the summer precipitation pattern in East China and the background circulation." Clim. Dyn., DOI: 10.1007/s00382-010-0852-9.

IntechOpen